In situ regeneration of nasal septal defects using acellular cartilage enhanced with platelet-derived growth factor

Huber Lena[1]*(iD), Gvaramia David[2]*(iD), Kern Johann[2], Jakob Yvonne[2], Zoellner Frank G[3], Hirsch Daniela[4], Breiter Roman[5](iD), Brenner Rolf E[6] and Rotter Nicole[1,2]

Abstract

Nasal septum defects can currently only be reconstructed using autologous cartilage grafts. In this study, we examine the reconstruction of septal cartilage defects in a rabbit model using porcine decellularized nasal septal cartilage (DNSC) functionalized with recombinant platelet-derived growth factor-BB (PDFG-BB). The supportive function of the transplanted DNSC was estimated by the degree of septum deviation and shrinkage using magnetic resonance imaging (MRI). The biocompatibility of the transplanted scaffolds was evaluated by histology according to international standards. A study group with an autologous septal transplant was used as a reference. In situ regeneration of cartilage defects was assessed by histological evaluation 4 and 16 weeks following DNSC transplantation. A study group with non-functionalized DNSC was introduced for estimation of the effects of PDFG-BB functionalization. DNSC scaffolds provided sufficient structural support to the nasal septum, with no significant shrinkage or septal deviations as evaluated by the MRI. Biocompatibility analysis after 4 weeks revealed an increased inflammatory reaction of the surrounding tissue in response to DNSC as compared to the autologous transplants. The inflammatory reaction was, however, significantly attenuated after 16 weeks in the PDGF-BB group whereas only a slight improvement of the biocompatibility score was observed in the untreated group. In situ regeneration of septal cartilage, as evidenced by the degradation of the DNSC matrix and production of neocartilage, was observed in both experimental groups after 16 weeks but was more pronounced in the PDFG-BB group. Overall, DNSC provided structural support to the nasal septum and stimulated in situ regeneration of the cartilage tissue. Furthermore, PDFG-BB augmented the regenerative potential of DNSC and enhanced the healing process, as demonstrated by reduced inflammation after 16 weeks.

Keywords

Decellularized matrix, nasal cartilage, in situ regeneration

[1]Department of Otorhinolaryngology, Head and Neck Surgery, University Medical Center Mannheim, Heidelberg University, Mannheim, Germany
[2]Department of Otorhinolaryngology, Head and Neck Surgery, Medical Faculty Mannheim, Heidelberg University, Mannheim, Germany
[3]Computer Assisted Clinical Medicine, Mannheim Institute for Intelligent System, Medical Faculty Mannheim, Heidelberg University, Mannheim, Germany
[4]Institute of Pathology, University Medical Center Mannheim, Heidelberg University, Mannheim, Germany

[5]Institute of Bioprocess Engineering, University of Erlangen, Erlangen, Germany
[6]Division for Biochemistry of Joint and Connective Tissue Diseases, Department of Orthopedics, University of Ulm, Ulm, Germany

*Both authors contributed equally.

Corresponding author:
Rotter Nicole, Department of Otorhinolaryngology, Head and Neck Surgery, University Medical Center Mannheim, University of Heidelberg, Theodor-Kutzer-Ufer 1-3, 68167, Mannheim, Germany.
Email: nicole.rotter@medma.uni-heidelberg.de

Graphical Abstract

In situ regeneration of nasal septal defects in rabbits using acellular cartilage enhanced with platelet-derived growth factor
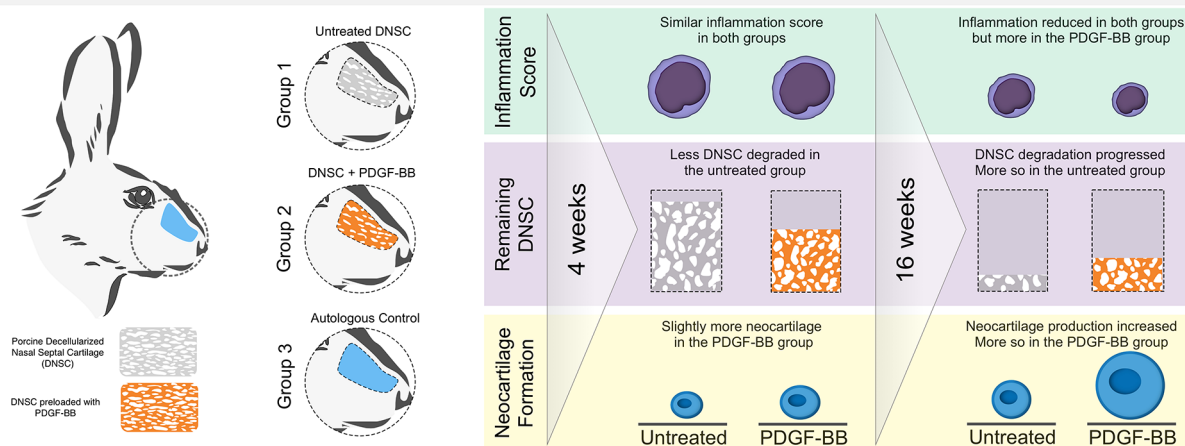
Introduction

Cartilage tissue does not regenerate easily and is difficult to replace when damaged due to trauma or infection. Defects of the nasal septal cartilage must often be reconstructed using auricular or costal cartilage grafts in complex surgeries, with the disadvantage of creating additional donor site morbidity. Using a tissue engineering approach, in situ tissue regeneration can be achieved by transplanting tailored biomaterials to the defect site to stimulate the recruitment of endogenous progenitor cells and subsequent replacement of the defect with the native tissue.[1] For this aim, biomaterials are functionalized with various chemotactic and morphogenic factors (e.g. peptides, cytokines).

In contrast to artificial biomaterials, decellularized extracellular matrices have the advantage of mimicking the composition, as well as the typographical architecture of the native tissues, which is too complex to be fully reproduced using a synthetic approach. Furthermore, the ECM of the acellular matrices can bind and sequester growth factors and cytokines, creating relevant gradients and providing necessary regenerative cues for the host cells.[2] Ultimately, the success of the decellularized scaffolds is determined by the degree to which the xenogeneic ECM can be remodeled and stimulate regeneration of the relevant host tissue after transplantation. On a larger scale, transplanted acellular scaffolds must provide a temporary supportive role at the place of the organ defect until the replacement of the ECM scaffold by the native tissue. This feature is specifically important for supportive structures, such as the nasal septum.[3,4]

In this study, we used porcine decellularized septal cartilage (DNSC) to stimulate the in situ regeneration of nasal septum defects in a rabbit model. The decellularization procedure of DNSC scaffolds has been previously established[5,6] and entails the removal of proteins, pathogenic agents, and reduction of glycosaminoglycans to obtain a xenogeneic porous collagen type II scaffold with structural similarity to the nasal septal cartilage. DNSC has demonstrated adequate mechanical properties and adaptability to different cartilage defects in vivo.[6,7] Furthermore, the rabbit animal model for nasal septum reconstruction used in this study has been previously established and DNSC has proven suitable for operative handling and preclinical analysis.[7]

Here we functionalized DNSC scaffolds by loading them with recombinant PDFG-BB, which has previously shown pronounced chemoattractant properties and strong potential for the recruitment of mesenchymal progenitors.[8,9] The in situ regeneration of cartilage defects in rabbit nasal septal cartilage was analyzed following the transplantation of cell-free DNSC-PDGF-BB constructs after 4 and 16 weeks, to evaluate early and late remodeling events.

Materials and methods

Production of decellularized porcine nasal cartilage scaffolds (DNSC)

DNSC scaffolds were prepared at the Institute of Bioprocess Engineering of the University of Erlangen, as previously described,[5,6] and supplied in a desiccated form. Endotoxin levels below 0.06 EU per mL were confirmed using PyroGene™ Recombinant Factor C Endotoxin Detection Assay (Lonza, Switzerland). To prepare the implants, the desiccated scaffolds were sliced into equal layers of 350 μm using a microtome (Leica RM2165) to match the approximate thickness of the rabbit nasal septum. The scaffolds were additionally sterilized by placing in EtOH 70% for 1 h prior to rehydration in Dulbecco's modified Eagle medium F-12 (DMEM F12) supplemented with 0.5% gentamicin and 10% heat-inactivated FBS (from here onward full cell culture medium) for 24 h at 37°C.

PDGF-BB uptake and release studies

To determine the most effective concentration for the preparation of PDGF-BB-laden DNSC, scaffolds from two different batches were incubated in triplicates in Petri dishes (3 cm) with different concentrations (0, 1, 2.5, 5, 10, and 20 µg/mL) of recombinant human PDGF-BB (rhPDGF-BB; Merck, Darmstadt, Germany) in FBS-free medium (DMEM/F12 1:1, Gibco) or in full cell culture medium for 24 h at 37°C on a plate shaker. Subsequently, DNSC scaffolds were examined for the presence of PDGF-BB by immunohistochemistry to determine the uptake of rhPDGF-BB.

The quantitative evaluation of PDGF-BB uptake and release was performed using an enzyme-linked immunosorbent assay (ELISA). To prepare the samples, 350 µm thick slices of DNSC were incubated in sterilized in EtOH 70% for 1 h and rehydrated in serum-free DMEM F12 supplemented with 0.5% gentamicin. The rehydrated scaffolds were then cut into 1 cm^2 pieces with a sterile scalpel and transferred to a 24-well plate, which was previously passivated with 10 mg/mL BSA (MilliporeSigma, Germany) for 1 h. Full cell culture medium with or without supplementation with PDGF-BB at concentrations of 5, 10, and 20 µg/mL (loading medium) was then added to the rehydrated scaffolds. In addition, a part of the DNSC samples was incubated in a PDGF-BB-free full cell culture medium (0 µg/mL rhPDGF-BB) to exclude the presence of PDGF-BB in the DNSC or medium components (e.g. FBS). After 24 h, the medium was collected into Eppendorf tubes previously passivated with 10 mg/mL BSA and stored at −80°C for later analysis. Aliquots of freshly prepared loading medium were also stored for analysis to confirm the exact concentration of the PDGF-BB solution applied to the DNSC. After loading with PDGF-BB for 24 h, the scaffolds were briefly washed to remove any residual cytokine before being transferred to another passivated 24-well plate and suspended in the full cell culture medium (release medium). The release medium was collected into passivated Eppendorf tubes after 3, 24, and 96 h and stored at −80°C until further analysis. Loading and release media from three independent experiments were then analyzed using Human PDGF-BB DuoSet ELISA (R&D systems, Bio-Techne). All reactions were performed in duplicate.

Migration assay

To examine the ability of rhPDGF-BB to induce migration of human nasal chondrocytes (ethics approval number: 2018-507N-MA) in cell culture medium and as a part of rhPDGF-BB-laden DNSC, the CytoSelect™ 24-Well Cell Migration Assay (Cell Biolabs, Inc., USA) was used according to manufacturer's instructions. Briefly, 5*10^5 human nasal chondrocytes from three different donors were resuspended in 300 µL FBS-free medium (DMEM/ F12 (1:1) (1X) + GlutaMAX™-I (Gibco), containing 0.05 mg/mL Gentamicin and seeded in the upper chamber (8 µm pore size) of a 24-well plate. 500 µL of full cell culture medium (DMEM/F12 (1:1) (1X) + GlutaMAXTM-I supplemented with 10% FBS and 0.05 mg/mL Gentamicin) was added to the lower well of the migration plate, containing DNSC scaffolds loaded with 0, 5, 10, or 20 µg/mL PDGF-BB. All wells were previously passivated with 10 mg/mL BSA to prevent adsorption of the released PDGF-BB to the cell culture plastic. A scaffold-free condition containing the full cell culture medium supplemented with 10 ng/mL PDGF-BB was included in each experiment as a positive control. After incubation for 24 h at 37°C and 5% CO$_2$, the medium was aspirated from the inside of the insert. Non-migratory cells were removed with a cotton swab moistened with PBS. The insert was placed in a clean well containing 400 µL of staining solution and incubated for 10 min at room temperature. The inserts were washed several times in water. For quantitative analysis, 200 µL of the extraction solution provided in the assay kit (Cell Biolabs Inc., USA) was added to an empty well. Then, the insert with migratory cells was placed in the extraction solution and incubated for 10 min on an orbital shaker. Subsequently, 100 µL of each sample was transferred to a 96-well microtiter plate and the absorbance was measured at 570 nm using a Tecan Infinite 200 Pro Plate reader. The ratio of the measured absorbance values relative to the control (PDGF-BB-free full culture medium) was used to estimate relative migration.

Animal model and surgical procedures

The use of 14–16 week-old female New Zealand white rabbits (Charles River Laboratories, Sulzfeld, Germany) for the animal experiments was approved by the regional authority in Karlsruhe (35-9185.81/G-46/20). The study groups were divided into three, consisting of four rabbits each: untreated DNSC was implanted in group 1, DNSC loaded with rhPDGF-BB was implanted in group 2, and the autologous septum transplantation was performed in group 3 (control). Two time points were chosen for the transplant analysis—the first evaluation was done after 4 weeks (short-term) and the second, after 16 weeks (long-term). The experiment involved 24 animals in total.

All surgeries were performed under sterile conditions using magnifying glasses. General anesthesia was induced by subcutaneous (s.c.) injection of Medetomidine (0.2 mg/ kg), Midazolam (1 mg/kg), and Fentanyl (0.02 mg/kg) (MMF mixture). Throughout surgery, narcosis was maintained by periodical (3–5 min, depending on the breathing frequency) intravenous (i.v.) injection through the ear vein of 0.1–0.2 mL MMF mixture diluted in NaCl 0.9% (1:3). The nasal area was shaved, and the skin was disinfected with Octenisept (Schuelke & Mayr GmbH, Germany). Then, an incision with a length of approximately 3 cm was made through the skin

and periosteum in the middle of the dorsum of the nose. A rectangle was marked on the bone, four holes were drilled at the corners of the rectangle with a diamond burr (diameter: 0.8 mm) and then connected using an osteotome. On one side, the bone was only weakened to allow for fracturing the bone to the side as a flap. The mucoperichondrium was dissected from the septal cartilage, and a piece of the cartilage of approximately 2 cm in length was carefully removed. The excised septal cartilage was then either replaced by a DNSC scaffold or re-implanted (autologous group). The scaffolds were cut to match the size of the removed septum and then measured in mm. The bone flap was replaced in its original position. The periosteum and skin were closed with sutures. Additionally, tissue adhesive (Surgibond, SMI) was applied to the skin after suturing. For details of the surgery, see Supplemental Figures (Figure S1).

For postoperative pain management, all animals were administered 0.05 mg/kg of Buprenorphine every 12 h. Wound healing and general health conditions were monitored daily. In case of inflammatory complications and signs of wound infection such as redness, swelling, or prolonged wound healing, the rabbits were treated with s.c. administration of Borgal 24% (Sulfadoxine/Trimethoprim) at a dosage of 15 mg/kg for three consecutive days. The weight of the rabbits was monitored regularly and supplemental feeding (critical care formula, Oxbow Animal Health, Omaha, USA) was provided in case of weight loss between 5% and 10% of the initial weight.

At the end of each experiment, the rabbits were euthanized under general anesthesia by i.v. injection of 400 mg/kg Pentobarbital through the ear vein.

MRI scanning

Immediately after euthanization, the heads of the rabbits were separated, skinned, and scanned using a 3T-MRI system (Magnetom Skyra, Siemens Heathcare Inc, Erlangen, Germany) using a 32 channel head coil to assess septal deviations, perforations, and shrinking of the scaffold. To depict the scaffold a 3D T1-weighted Sampling Perfection with Application optimized Contrasts using different flip angle Evolution (SPACE) sequence with parameters echo time (TE)=9.1 ms, repetition time (TR)=900 ms, flip angle (FA)=120° was used. The field of view was set to 90×180 mm^2 and a matrix of 96×192 (reconstructed to 192×384 by tero filling) resulting in an isotropic resolution of 0.5 mm^3. Parallel imaging of factor 2 and 4 averages were used. In total 104 slices in coronal orientation were recorded. Total acquisition time was 6 min and 14 s. In addition, a 3D T2-weighted SPACE sequence was acquired with TE=410 ms, TR=3200 ms. All other sequence settings were kept as for the T1-weighted sequence, except FOV=189×189 mm^2 and matrix=192×92, reconstructed to 384×384 also resulting in the same isotropic resolution of 0.5 mm^3. Images were recorded in sagittal orientation. Total

acquisition time was 4 min and 38 s. After image acquisition, the sagittal T2-weighted images were reformatted to coronal slice orientation. The septum length was measured in the MRI images and compared to the intraoperative measurement of transplant length for the assessment of septum shrinkage.

Histology and immunohistochemistry

After MRI, the entire nose was detached from the skull with an electric diamond blade saw. The nose was then decalcified with 0.7 M ethylenediamine tetra-acetate (EDTA) in 4% formalin pH 7.4 for 6 weeks. Afterward, the whole nose was cut into three parts and embedded in paraffin. Paraffin sections (5–7 µm) were stained with Hematoxylin and Eosin (H&E) using standard protocols. Alcian blue staining was performed to visualize sulfated GAGs by immersing the paraffin sections into 1% Alcian blue solution in 3% acetic acid (pH 2.5) for 30 min at RT. The sections were then transferred to 3% acetic acid for 1 min and subsequently washed in distilled H$_2$O for 2 min before being counterstained with 0.1% nuclear fast red (Sigma).

For immunohistochemistry (IHC), paraffin sections were subjected to antigen retrieval with citrate buffer pH 6.0 at 80°C for 20 min. The sections were then incubated with Proteinase K (Dako, Agilent, Germany) for 6 min and subsequently with endogenous peroxidase blocking solution (Dako, Agilent Technologies, Germany) for 30 min. After blocking with 10% normal sheep serum for 30 min, the sections were incubated with a primary antibody against collagen type II (CIIC1, DSHB, IA, USA) 1:100, or collagen type I (NB600-450, Novus Biologicals, Germany) 1:100 at 4°C overnight. The sections were then washed in PBS 0.1% Tween 20, and the secondary antibody (biotinylated anti-mouse IgG, Thermo Fisher Scientific) was added for 45 min. The samples were washed prior to the application of streptavidin-biotinylated horseradish peroxidase complex (GE Healthcare) and visualized with 3-Amino-9-ethylcarbazole (AEC) peroxidase substrate solution (ScyTek Laboratories, Germany).

To confirm the loading of DNSC with PDGF-BB, the treated scaffolds were processed for immunohistochemistry as described above and a primary antibody against PDGF-BB (Cat. # 07-1437, Merck, Darmstadt, Germany) 1:200 was used for staining.

All tissue sections were evaluated using Zeiss Axio Observer and micrographs were acquired using Zeiss Axiocam 503 (both Carl Zeiss Microscopy GmbH, Germany).

Evaluation of biocompatibility

The assessment of in vivo biocompatibility of all DNSC scaffolds and the autologous control was performed according to ISO 10993-6:2016 of the biological assessment of medical

devices (Biological evaluation of medical devices—Part 6: Tests for local effects after implantation). Histological characteristics, such as encapsulation, presence of polymorphonuclear leukocytes, lymphocytes, plasma cells, macrophages, and giant cells, along with necrosis, neovascularization, fatty infiltration, and fibrosis were assessed using a semi-quantitative approach. Based on these histological parameters, the score was then calculated and the autologous control was subtracted from all conditions to obtain the final score. The degree of irritation was then classified as minimal (0–2.9 points), slight (3–8.9 points), moderate (9–15), or strong (>15.1), according to the ISO standard.

Quantitative image analysis

Panoramic images of the entire paraffin sections stained with Alcian blue were processed using ZEN software version 2.3 (Carl Zeiss Microscopy GmbH) by marking the total sample area and areas of neocartilage and the remaining DNSC using a spline contour tool (Supplemental Figure S6 (A) and (B)). Neocartilage was defined based on the Alcian blue staining and characteristic tissue morphology. The summed area of neocartilage or DNSC was then normalized against the total sample area of the respective section.

Statistics

Nasal septum deviation measurements from MRI images were compared by ANOVA followed by Dunnett's multiple comparisons test. The results of the quantitative image analysis were analyzed using One-Way ANOVA followed by Tukey's Multiple Comparison Test. Statistical analyses were performed using GraphPad Prism Software Version 5.03 (CA, USA). Significance was denoted as follows: $*p < 0.05$, $**p < 0.01$.

Results

Loading of DNSC scaffolds with PDGF-BB

Concentrations of up to 2.5 μg/mL PDGF-BB did not result in detectable staining (data not shown). Incubation with a concentration of 5 μg/mL rhPDGF-BB showed weak staining of rhPDGF-BB within the scaffold while the use of a 10 and 20 μg/mL rhPDGF-BB solution showed strong staining of adsorbed rhPDGF-BB throughout the entire scaffold, albeit no pronounced difference in the staining intensity was observed between the two higher loading concentrations (Figure 1(a)). In addition, loading of the scaffolds was only effective in the presence of FBS in the loading medium. The previous in vivo study has shown that FBS did not affect the inflammatory response in rabbits.[7] Therefore, a loading medium supplemented with 10% FBS was used to produce rhPDGF-BB-laden scaffolds in all further experiments.

By quantitative analysis with ELISA, 29% of the initial PDGF-BB was recovered following a 24 h incubation of the DNSC with 20 μg/mL cytokine, corresponding to uptake of 71% (Figure 1(b) and (c)). Similarly, PDGF-BB uptake of 68% was observed following the loading with 10 μg/mL cytokine. With 5 μg/mL loading, the uptake was reduced to 62%.

Release of PDGF-BB and the migratory response of nasal chondrocytes

To estimate the amount of release, scaffolds loaded with 5, 10, and 20 μg/mL PDGF-BB were incubated for 4 days in the full cell culture medium with no further cytokine supplementation. The medium was collected after 3, 24, and 96 h for quantitative analysis of PDGF-BB release from the DNSC. Cumulative cytokine release after 96 h correlated with the degree of loading, corresponding to 1.1 (±0.2) μg/mL after loading with 5 μg/mL, 1.8 (±0.2) with 10 μg/mL, and 3.4 (±0.2) with 20 μg/mL PDGF-BB (Figure 1(d)). A sustained release of the cytokine was observed in scaffolds with 5 and 10 μg/mL loading during the period of the experiment. Particularly, release after 5 μg/mL loading constituted an average of 0.3 μg/mL after 3 h and 0.4 μg/mL after 24 and 96 h. From scaffolds functionalized with 10 μg/mL PDFG-BB, 0.6 μg/mL average release was detected at each time point. In contrast, release from DNSC functionalized with 20 μg/mL PDFG-BB increased from 1.1 μg/mL at 3 h to 1.5 μg/mL at 24 h and reduced to 1.0 μg/mL at 96 h, showing a slight tendency to decrease during the period of analysis. No PDFG-BB was detected in the control condition incubated with a PDGF-BB-free full cell culture medium.

The migration assays showed that scaffolds loaded with 10 and 20 μg/mL PDFG-BB induced migration of human nasal chondrocytes comparable to the positive control (medium containing soluble PDGF-BB) (Figure 1(e)), whereas no or negligible migration was observed in untreated scaffolds or DNSC loaded with 5 μg/mL. A comparable degree of migration was induced by DNSC loaded with 10 and 20 μg/mL PDFG-BB, with 10 μg/mL loading leading to even a slightly more pronounced migration of chondrocytes as compared to the 20 μg/mL. Notably, a considerable PDGF-BB-induced increase in chondrocyte migration was only observed in presence of FBS in the medium. Due to the efficiency of migratory activity, as well as the stable cytokine release, DNSC functionalized with 10 μg/mL was used further in the animal experiments.

General reactions to surgeries

One rabbit showed signs of a back injury before the start of the experiments and one rabbit died from apnea during anesthesia. These animals were excluded from the study.
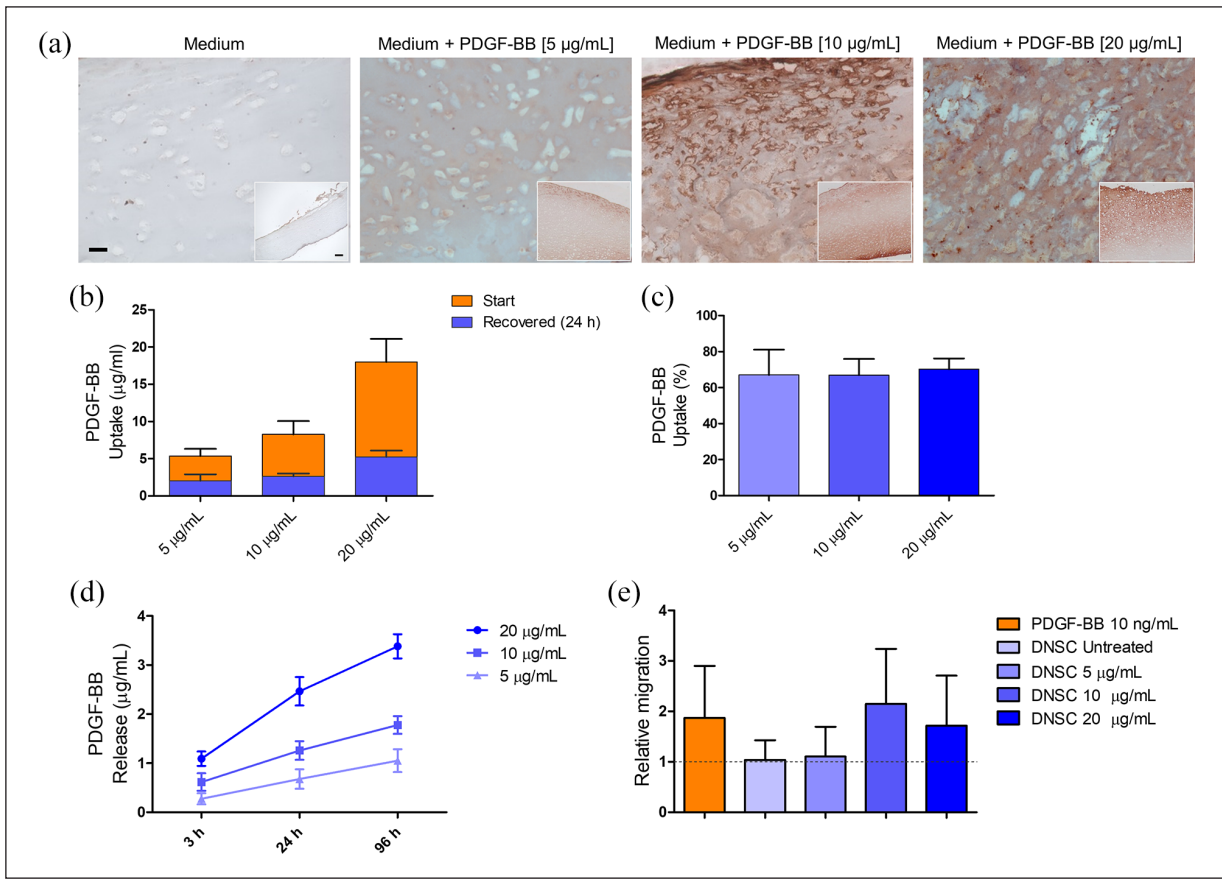
Figure 1. Loading, release, and migration studies with rhPDGF-BB-laden DNSC scaffolds. (a) DNSC scaffolds were incubated with cell culture medium with or without rhPDGF-BB (5, 10, and 20 μg/mL) for 24 h at 37°C. Immunohistochemistry stainings for PDGF-BB showed no staining in the DSNC incubated with medium alone, a weak staining with medium supplemented with 5 μg/mL rhPDGF-BB, and a strong staining with medium supplemented with 10 and 20 μg/mL rhPDGF-BB. However, qualitatively no substantial difference was not observed in the staining intensity between 10 and 20 μg/mL loading. Scale bar 50 μm; Insets depict an overview image of the respective DNSC scaffold (Scale bar 100 μm). (b) Uptake following the loading of DNSC scaffolds with 5, 10, and 20 μg/mL of rhPDFG-BB displayed as the concentration of the recovered cytokine after 24 h and (c) percentage of uptake. (d) The release of rhPDGF-BB loaded with different concentrations of the cytokine after 3, 24, and 96 h. (e) DNSC scaffolds loaded with 10 and 20 μg/mL, but not 5 μg/mL PDGF-BB induced migration of nasal chondrocytes similar to the positive control (10 ng/mL PDFG-BB in full cell culture medium). Migration relative to the control (the full cell culture medium without cytokine supplementation, dashed line) is shown. All data depicted as mean ± SD of three experiments.

Two rabbits (group 1 and group 3) developed signs of post-operative wound infection and were successfully treated with antibiotics (Borgal 15 mg/kg). Four rabbits lost between 5% and 10% of their initial weight after surgery, which was successfully restored by supplemental feeding. None of the animals showed breathing difficulties or epistaxis.

MRI measurements

The length of the septum and the angle of septum deviation were measured in the axial MRI planes. The measured septum length was then compared to the intraoperative measurement of the transplants to assess transplant shrinkage. The re-implanted autologous septum and DNSC transplants were similar in thickness and morphology and were indistinguishable on the MRI images (Figure 2). No

septal perforations were detected in any of the experimental animals. Furthermore, no significant transplant shrinkage was observed in any study group after 4 or 16 weeks. In some animals, irrespective of the study group, minor septal deviations occurred mostly at the anterior end of the septum (Figure 2). However, no significant differences in the mean septal deviation were observed between the scaffold groups (1 + 2) and the control group (3). Mean septum deviations, as well as the differences between intraoperative transplant length and MRI measurements, are summarized in Table 1.

Biocompatibility of DNSC and PDGF-BB-laden scaffolds

A slight degradation of DNSC scaffolds was observed on the H&E samples after 4 weeks in both experimental
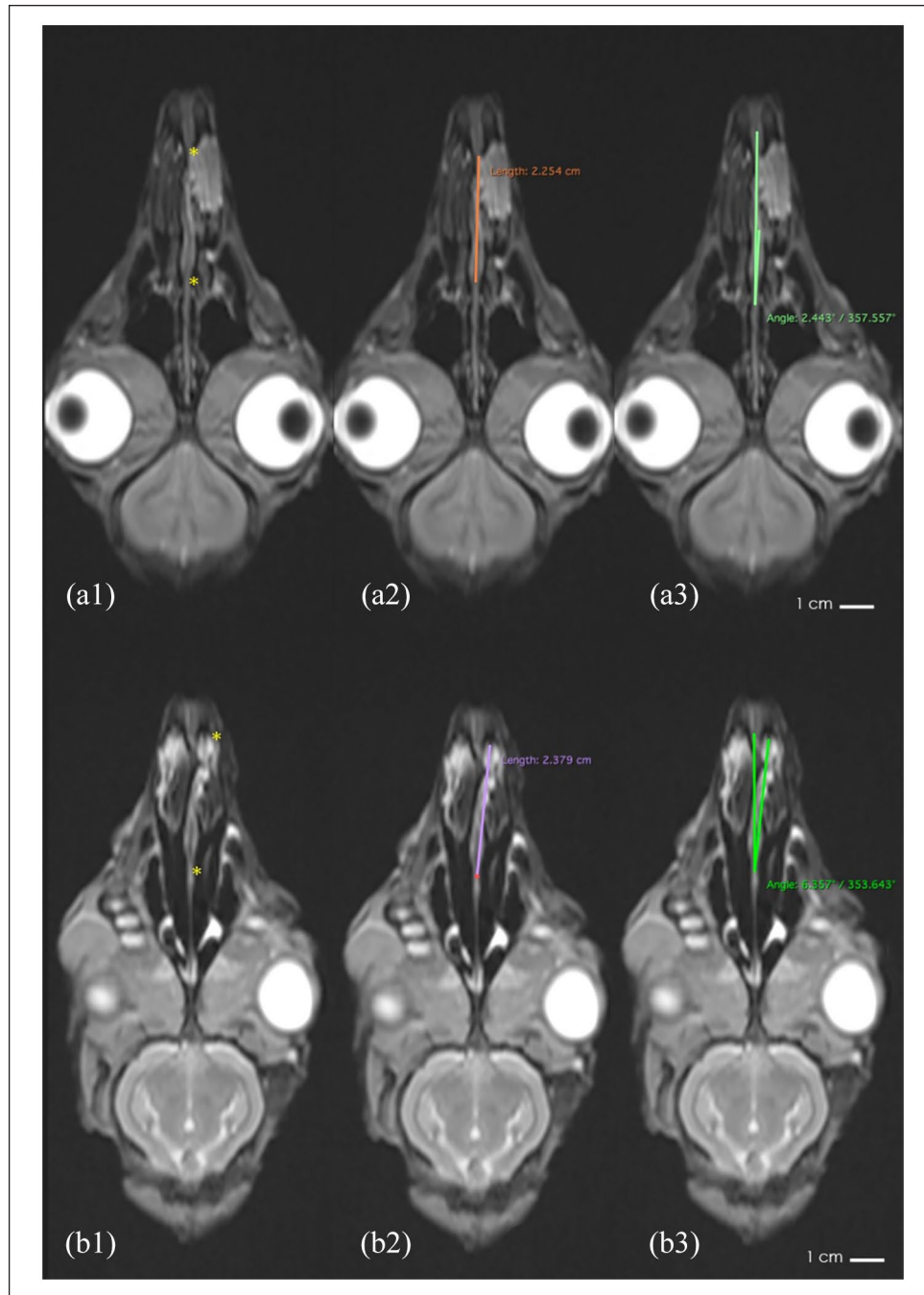
Figure 2. MRI scan of rabbit skulls. (a) MRI head scan of an autologous control after 16 weeks and (b) an implanted PDGF-BB-scaffold after 4 weeks. a1/b1: The asterisks mark the anterior and posterior end of the reimplanted autologous septal cartilage (a1) or DNSC (b1). An example of septum length measurement used for comparison with the intraoperative length measurements of the transplants is shown in (a2 and b2) a3 and b3 depict the measured deviation of the septum at the approximate location of the transplant relative to the rest of the septum. Note that the deviation often occurs at the anterior end where the scaffold does not align with the rest of the septum.

groups (Figure 3(b)). The surrounding inflammatory cells, mostly lymphocytes, started to infiltrate the scaffold from the borders. The cartilage of the autologous control did not show any signs of degradation after 4 or 16 weeks (Figure 3(a)). Small islets of neocartilage were found in

the areas between the scaffold and the mucoperichondrium (Figure 3(b)).

The experimental groups (1 and 2) showed a reaction to the implanted scaffolds in comparison to the autologous control group in both short-term (4 weeks) and long-term

Table 1. Shrinkage and septum deviations in the MRI head scans. The differences between the lengths of the transplants measured intraoperatively and on the MRI image are shown. Septum deviation was measured as the angle between the scaffold and the rest of the septum. Values are shown as mean ± SD. No significant differences were seen in either scaffold length or the septum deviation in comparison to the autologous control.

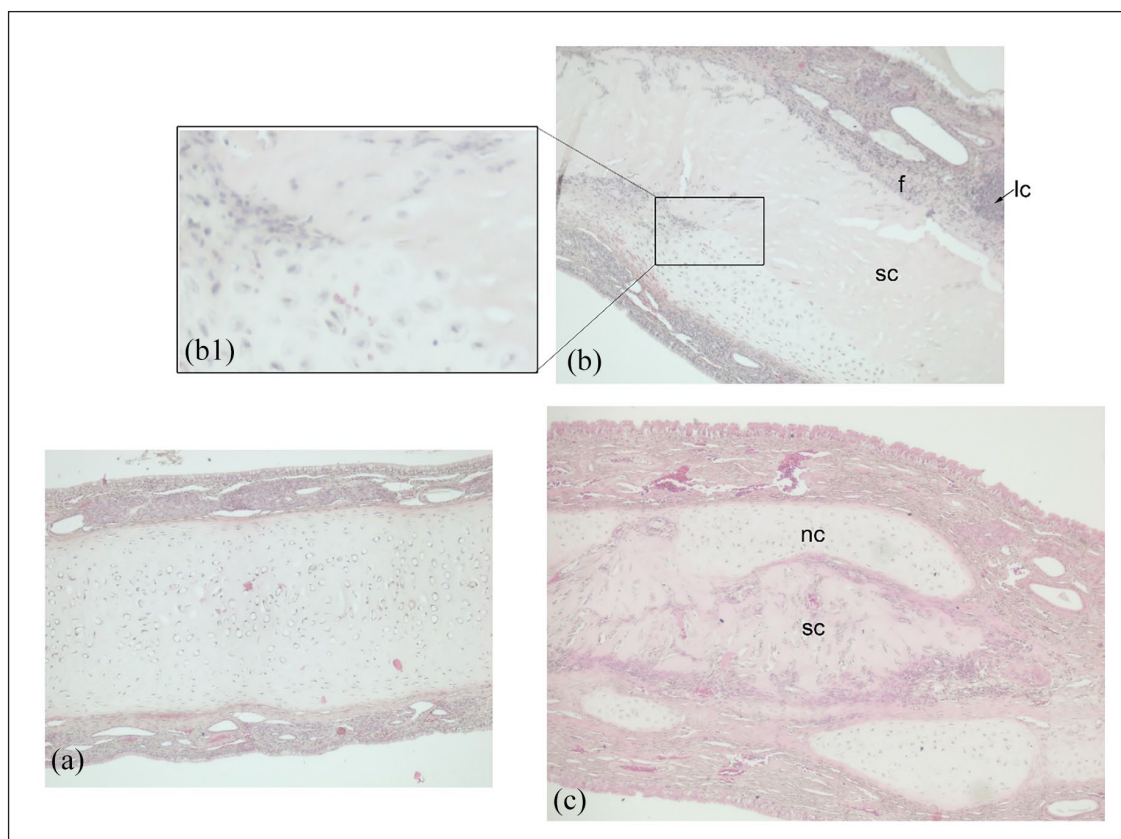| Timepoint	Study group	Length difference (cm)	Septum deviation
4 Weeks	Untreated	0.15 ± 0.13	5.1° ± 8.58°
	PDGF-BB	0.09 ± 0.04	1.94° ± 0.96°
	Autologous control	0.06 ± 0.02	4.02° ± 3.9°
16 Weeks	Untreated	0.11 ± 0.09	3.52° ± 5.9°
	PDGF-BB	0.07 ± 0.06	1.08° ± 1.42°
	Autologous control	0.25 ± 0.2	3.83° ± 1.73°

Figure 3. Morphology of implants. (a) The reimplanted autologous septum (group 3) after 4 weeks is intact, the mucosa tightly attached to the septum and only few signs of inflammatory reaction are seen. (b) After 4 weeks of implantation, partial degradation of the scaffold, lymphocyte infiltration, fibrosis, and islets of neocartilage formation are observed at the scaffold periphery. Mesenchymal cells and lymphocytes start to infiltrate the scaffold. Non-functionalized scaffold (group 1) is shown on the representative image. (c) After 16 weeks, degradation of the scaffold is more pronounced, the infiltrating cells have penetrated the scaffold fully and more neocartilage is visible. The representative image depicts scaffolds from group 2.
f: fibrosis; sc: scaffold; nc: neocartilage; lc: lymphocyte infiltration.

(16 weeks) experiments (Table 2). When normalized to the autologous control, however, the scores amounted to slight irritation (3–8.9 points), as classified by the aforementioned DIN norm (see Materials and methods). Lymphocyte infiltrations of varying thickness were found in all groups but considerably less so in the control group (Figure 3). Other inflammatory cells such as plasma cells, macrophages, and

polymorphonuclear cells were also more frequently detected in the scaffold groups. Neovascularization was present in all groups; tissue necrosis was not present in any of the samples. Remarkably, the inflammatory reaction in the PDGF-BB group was significantly reduced (p=0.025) after 16 weeks as compared to 4 weeks, whereas no significant change in the biocompatibility score was observed in study

groups 2 and 1 (Table 2). Furthermore, fibrosis, neovascularization, and fatty infiltration were also less pronounced after 16 weeks in the PDFG-BB group.

Remodeling of the DNSC matrix

After 4 weeks, initial signs of scaffold degradation and infiltration of the matrix with immune cells were visible in both untreated and PDGF-BB groups. However, the overall shape of DNSC transplants was retained with the structure uninterrupted across the whole span of the nasal septum (Supplemental Figure S3). The degradation of the matrix, as well as production of the new cartilage tissue, was observed predominantly in the ventral parts of the septum, in the vicinity of the degrading DNSC matrix (Supplemental Figure S3). Some cartilage tissue remaining after the resection of the septal cartilage was often visible on the ventral side of the septum with islets of neocartilage forming in the space between DNSC and the remaining septal cartilage. Neocartilage formation was usually surrounded by cellular infiltrates and could be differentiated from the mature cartilage morphologically by smaller lacunae, higher Collagen type I (Col1) staining, and low or absent Collagen type II (Col2) staining (Supplemental Figure S3). However, positive Alcian blue staining and characteristic cartilage tissue morphology were already visible and used as the main criterion for the identification of neocartilage.

In some instances, neocartilage formation was also detected laterally at the transplant-perichondrium interface, sometimes fusing with the DNSC matrix (Supplemental Figure S4). No neocartilage formation from perichondrium was seen in the autologous control groups (Supplemental Figures S2 and S5). Autologous transplants mostly healed well with very little immune cell infiltration and no signs of fibrotic tissue at the resection site.

Quantitative analysis of all histological samples from the 4 week samples did not reveal any significant differences in the formation of neocartilage between the PDGF-BB and the untreated group (Figure 5(b)). There was somewhat less DNSC per total section area in the PDGF-BB groups as compared to the untreated samples, however, the difference was not significant.

After 16 weeks, degradation of DNSC was apparent in both PDGF-BB and the untreated groups (Figure 4). The structural integrity of the matrix was no longer retained and only disconnected regions of DNSC surrounded by neocartilage, cellular infiltrates, and/or fibrous tissue were observed in most sections. As in the short-term samples, the fusion of neocartilage and DNSC matrices was sometimes visible (Figure 5(a)). However, unlike the 4 week samples, in long-term samples, most of the DNSC lacunae were infiltrated by the host cells at the place of matrix fusion, signifying an active reorganization of the DNSC matrix (Figure 5(a)).
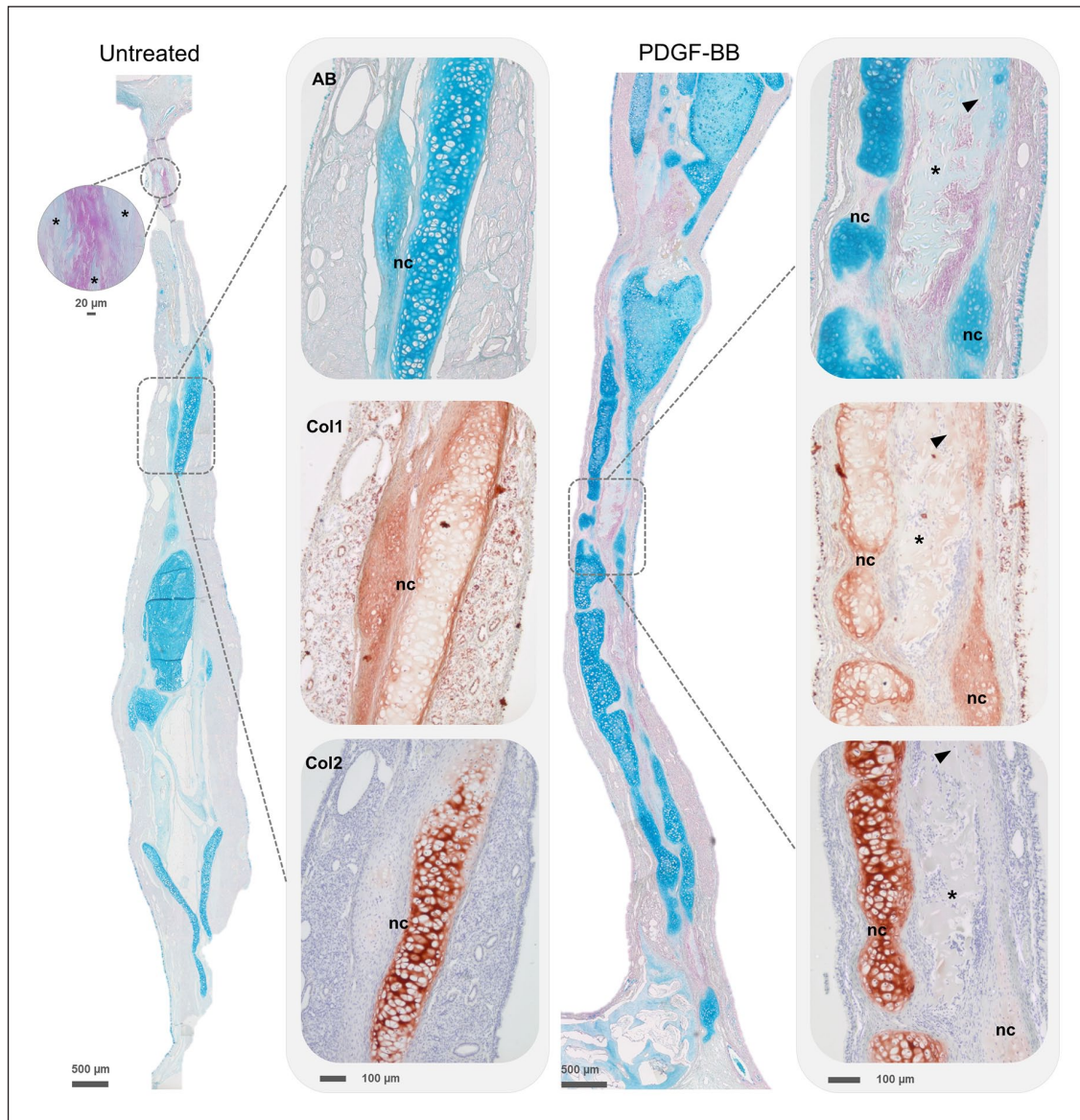
Table 2. Evaluation of biocompatibility. Biocompatibility scores of groups 1–3 are shown as mean ± SD.

Time-point	Group	PMNC	LC	PC	Macrophages	Giant cells	Necrosis	NV	Fibrosis	Fatty infiltrate	Score
4w	Untreated	1.33 ± 0.58	3.33 ± 0.58	1.67 ± 0.58	1 ± 0	0.33 ± 0.58	0	1.67 ± 1.15	1 ± 0	0.67 ± 0.58	8.67
	PDGF-BB	1.5 ± 0.58	2.75 ± 0.5	1.25 ± 0.5	1 ± 0	0.25 ± 0.5	0	2 ± 0	1.75 ± 0.96	1.25 ± 0.5	8.5
	Control	0.75 ± 0.5	1 ± 0	1 ± 0	0	0	0	2 ± 1.15	1.75 ± 0.5	0.75 ± 0.5	-
16w	Untreated	2 ± 0	3 ± 0.82	1 ± 0	0.75 ± 0.5	0	0	1.75 ± 0.5	1.5 ± 0.58	1 ± 0.82	6.75
	PDGF-BB	1.25 ± 0.5	2.5 ± 0.58	1 ± 0	1 ± 0	0	0	1 ± 0	1.5 ± 0.58	0.5 ± 0.58	3.5*
	Control	0.67 ± 0.58	1 ± 0	0.33 ± 0.58	0.33 ± 0.58	0	0	3 ± 0	1 ± 0	0.33 ± 0.58	-

The asterisk in the PDGF-BB group marks a significant change in inflammation after 16 weeks as compared to 4 weeks (*$p < 0.05$). The scores are shown relative to the autologous control (autologous control subtracted from the initial score).
PMNC: polymorphonuclear cells; LC: lymphocytes; PC: plasma cells; NV: neovascularization.

Figure 4. Immunostaining of DNSC transplants. Representative immunostaining of nasal septum from groups 1 and 2 after 16 weeks. Note the differential staining against Col1 and Col2 in the newly produced and more mature cartilage tissues. The arrowheads indicate the regions of fusion between DNSC (*) and neocartilage (nc). Staining denoted as follows: AB: Alcian Blue; Col1: collagen type I; Col2: collagen type II.

Quantification of the histological images from the 16 week samples of group 1 revealed >5-fold decrease in the amount of DNSC as compared to the short-term samples (Figure 5(b), right panel). In contrast, more DNSC could be detected in the PDGF-BB samples, with a relatively minor reduction of <2-fold in the total amount of the matrix as compared to the 4 week samples of the PDFG-BB group. Quantitative comparison of neocartilage formed in the two long-term animal groups also revealed significant differences with the PDGF-BB group showing >4-fold increase in the mean amount of neocartilage per total area as compared to the short-term samples (Figure 5(b), right panel). In contrast, only a 1.7-fold increase in the production of neocartilage was

seen in the 16 week samples of group 1 compared to the 4 week samples.

Overall, an inverse correlation between the newly produced cartilage and the amount of DNSC was observed in both groups after 16 weeks (Supplemental Figure S6 (D)). However, the correlation between DNSC degradation and chondrogenesis was less pronounced in group 2 after 16 weeks, with more neocartilage produced but less DNSC degraded as compared to the untreated samples.

Discussion

In this study, we analyzed in situ regeneration of nasal septal cartilage defects after transplantation of a decellularized
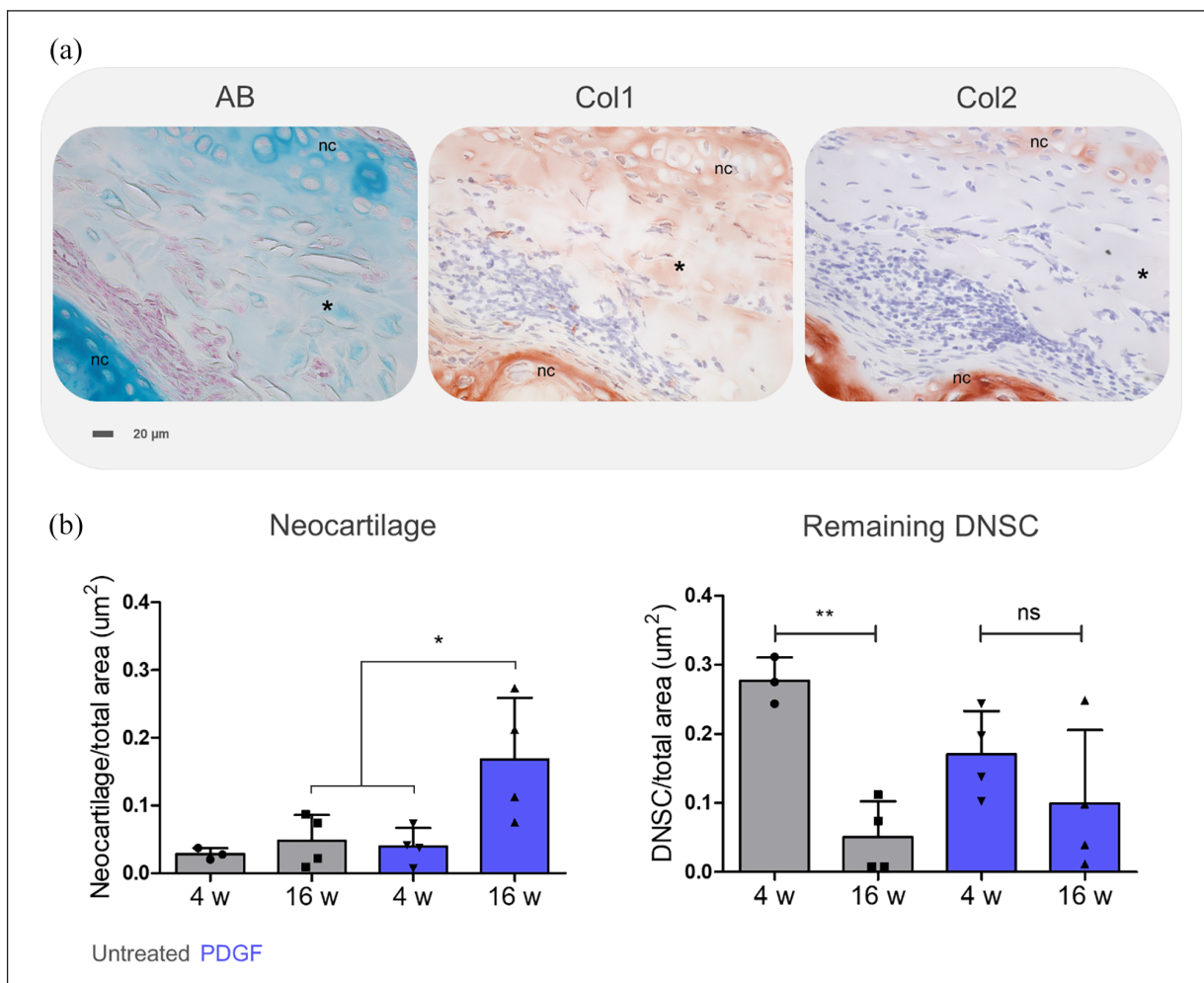
Figure 5. Formation of neocartilage and degradation of DNSC. (a) Regions demonstrating fusion between DNSC (*) and neocartilage (nc) in the PDGF-BB group after 16 weeks. Note the infiltration of mesenchymal cells actively reorganizing the matrix and penetrating the DNSC lacunae. AB: Alcian Blue; Col1: collagen type 1; Col2: collagen type 2. (b) Quantification of sum area of the neocartilage (left) or DNSC remnants (right) versus total area of the histological section. The differences between the neocartilage or the remaining DNSC between the 4 week untreated and PDGF-BB groups are not significant. Data mean ± SD, *$p < 0.05$, **$p < 0.01$, 1-way ANOVA.

cartilage matrix functionalized with PDGF-BB. The matrix used in the study has been previously established and shown promising results in vitro, as well as in vivo in a rat model causing only minor inflammation and preventing septal perforations.[10] More importantly, the material has already been used in the rabbit model using a similar transplantation approach[7] as described in this study. The major difference between the two studies is that in the previous study[7] scaffolds were seeded with autologous chondrocytes derived from the auricle. Comparable to the rat study, this previous in vivo work in rabbits also showed good long-term biocompatibility of the matrix with only moderate irritation. However, only limited regeneration of the septal cartilage was observed. Specifically, the seeding of the matrix with autologous auricular chondrocytes did not enhance chondrogenesis after 6 months. Rather, a deformation of the DNSC scaffolds with subsequent septal deviations occurred, and seeding even negatively affected the biocompatibility of the scaffold, leading to an increase in irritation, although, both seeded and unseeded matrices were able to prevent septal perforations.

Therefore, in this follow-up study, we focused on the in situ regenerative strategy as opposed to using autologous cells. In contrast to the ex vivo tissue engineering, which employs cell-laden biomaterials, the in situ approach takes advantage of the innate regenerative potential of the organism using biophysical and biochemical cues to recruit resident progenitors or to skew the immune response toward a pro-remodeling process.[1] The in situ approach thus removes the need for an additional biopsy, which is required for obtaining autologous cells and leads to donor site morbidity. Furthermore, the risks associated with the

ex vivo manipulation and expansion of the cells, such as contamination and dedifferentiation, are eliminated. In addition, time-consuming in vitro cultivation of cells is avoided, which is a clear clinical advantage. In situ tissue engineering has found use in cartilage regenerative therapy, particularly in articular cartilage sites, where reconstructive procedures often rely on the recruitment of bone marrow MSCs from the subchondral bone. This cell-free approach is often combined with microfracture of the subchondral bone to enhance mobilization of the resident MSCs.[11,12] The engineering strategies vary from a chemical modification of biomaterials with peptides, which stimulate MSC recruitment[13,14] to modification with chemotactic factors, such as SDF-1[15] and chondrogenic factors, such as TGF-β1.[16]

In non-articular cartilage defect sites, the recruitment of mesenchymal progenitors may be problematic due to the inherent scarcity of endogenous cells.[1] In this study, we chose the approach of functionalization of the DNSC scaffold with PDGF-BB to enhance the in situ regenerative properties of the matrix through the active recruitment of endogenous progenitors. PDGF-BB is a versatile growth factor known for its activity as a mitogen and a chemotactic agent in cells of mesenchymal origin stimulating their recruitment and proliferation.[17,18] It is known to enhance migration in mesenchymal[8] and chondrogenic progenitor cells.[19] In our study, we observed an efficient uptake and stable release of PDGF-BB from the DNSC scaffold. Furthermore, functionalized scaffolds demonstrated induction of chemotactic activity in nasal chondrocytes in vitro, confirming that the chemoattractant property of PDFG-BB was retained after binding and release from the DNSC scaffold. Consistently, significantly higher neocartilage production originating from the perichondrium and neighboring cartilage was observed in vivo in the experimental groups with functionalized DNSC scaffolds.

However, it should be mentioned that the concentration of the released cytokine did not correlate to the degree of migration in our in vitro experiments. There was a negligible response of chondrocytes to the DNSC loaded with 5 μg/mL PDFG-BB, whereas release of the cytokine with the given loading concentration was as much as 0.3 μg/mL already after 3 h, as detected by ELISA. In contrast, 10 ng/mL soluble PDGF-BB in the control condition effectively induced chondrocyte migration. An enhanced migration caused by PDGF-BB-laden DNSC was only seen at 10 μg/mL loading, with no further increase (and even slight reduction) of induced chemotactic activity by the scaffolds loaded with 20 μg/mL PDGF-BB. The effectiveness of 10 versus 20 μg/mL loading could be explained by the saturation of chemotactic response in chondrocytes. However, the cause of the discrepancy between the amount of released PDFG-BB and chemotactic activity is unclear. There is a possibility that partial loss of PDGF-BB chemoattractant property occurs after the reversible binding of the cytokine

to the DNSC matrix due to a conformational change in the protein structure. However, reports of the loss of biological activity following PDGF-BB adsorption are uncommon.[20,21] A more likely explanation might be that the formation of an effective cytokine concentration gradient does not occur in the static conditions of the in vitro migration assay setting. The majority of the released cytokine might be remaining in the immediate vicinity of the scaffold with only a small fraction reaching the contact area between the surface of the medium and the migration chamber. In contrast, PDFG-BB in the soluble control is sufficiently mixed and readily available to the cells within the chamber.

Due to its pleiotropic effects, localized sustained delivery of PDGF-BB has found regenerative applications in wound healing,[22] prevention and regeneration of myocardial infarction,[23,24] treatment of diabetic ulcers,[25] and repair of bone defects.[26] Recombinant PDGF-BB causes significant acceleration of wound healing through recruitment and activation of fibroblasts and macrophages to the wound site and induces a positive autocrine feedback loop leading to further PDFG-BB synthesis by the recruited cells.[27] Furthermore, PDGF-BB has been reported to enhance the deposition of ECM components such as hyaluronic acid and collagens in fibroblasts[27] and types of articular cartilage.[28] Lastly, PDGF-BB suppresses IL-1β-induced cartilage degradation and chondrocyte apoptosis.[29] Together, these factors could explain the enhanced formation of neocartilage, as well as the rapid decrease in an inflammatory reaction in the PDGF-BB-loaded group after 16 weeks.

Besides functionalization of materials with chemotactic agents for the recruitment of endogenous cells to the defect site, an indirect strategy of in situ engineering is to render materials with immunomodulatory properties and stimulate a pro-remodeling immune response after transplantation.[30] Synthetic non-degradable materials typically progress into an unresolved inflammatory response, which culminates in the formation of the avascular fibrous capsule.[31] To prevent thick capsule formation, strategies such as coating non-degradable materials with antifouling polymers (e.g. zwitterionic elastomers) or functionalization of scaffolds with anti-inflammatory factors are employed.[32–34] In contrast to the synthetic materials, ECM-based transplants are inherently susceptible to proteolytic degradation if no further crosslinking has been applied during the decellularization procedure. Degradability of the ECM materials combined with their natural chemical composition is hypothesized to enhance remodeling of the transplantation site through immune modulation.[35,36] The proposed mechanisms of this process are the production of cryptic peptides—hidden residues in the ECM that elicit their biological activity after proteolytic degradation of the parent molecule.[2,37] In addition, degradation stimulates the release of the ECM-tethered growth factors and matrix-bound vesicles containing bioactive signaling molecules

(e.g. lipids and microRNA).[38] Synergistically, these factors are thought to stimulate regeneration of the host tissue by modulating the immune response and promoting the activity of relevant progenitor cells.[36,38] Collectively, this process has been termed constructive remodeling to differentiate it from the conventional foreign body response. In an ideal case, remodeling of the decellularized matrix culminates in the complete regeneration of the native tissue, as opposed to the fibrous process and formation of the collagen capsule or scar tissue.

Reconstruction of septal defects in a rabbit model using synthetic matrices, such as Gore-Tex and Dacron display a response characteristic for the FBR, leading to inflammation and deposition of fibrous tissue as opposed to chondrogenesis.[39] DNSC matrix used in our study is non-crosslinked and fully degradable. Consistent with the hypothesis of constructive remodeling, neocartilage in the histological sections is often found at the site of active DNSC degradation and reorganization in both untreated and PDGF-BB groups. Cellular infiltrates around the degraded DNSC, and at later time points, inside the DNSC lacunae, are also suggestive of the remodeling process. Neochondrogenesis originating from the perichondrium is seen in both DNSC groups but not in the autologous group. Often, ECM of the newly formed cartilage directly fuses with DNSC, suggestive of some stimulatory effect of the matrix. Furthermore, we see a correlation between degradation of DNSC and formation of neocartilage (i.e. negative correlation between the amount of DNSC and neocartilage present) after 16 weeks. Finally, consistent with the immunomodulatory effects of the matrix degradation products, all of the groups in our experiments displayed signs of a moderate inflammatory response, which regressed significantly after 16 weeks as the matrix degradation progressed.

While the in situ degradation of the ECM scaffold is desired for constructive remodeling, it is important that degradation does not occur prematurely and is matched with the pace of the remodeling process.[1] This is especially crucial for anatomical structures, which primarily carry a supportive function, as is the case with some anatomic areas of the nasal septum.[4] The decellularization procedure was reported to reduce the stiffness of the native porcine nasal septum by up to 69.5%.[6] Therefore, retention of the supportive function after decellularization was particularly important for this study. Importantly, DNSC was able to take over the supportive function with the overall scaffold integrity still retained after 4 weeks. The analysis of the MRI scans did not show a significant shrinking of the scaffold length. Consistently, no shrinking of the implants was found in the previous study.[7] We found septal deviations in all groups and at all time points mostly at the anterior end of the scaffold suggestive of a misalignment of the scaffold with the remaining septum, probably caused by the imprecise positioning of the scaffold. These deviations were, however, minor and did not cause breathing difficulties. The scaffolds thus seem to provide sufficient structural support as a replacement of the nasal septum until the remodeling process is complete. After 16 weeks, no relevant septum deviation was measured in the MRI images. This suggests that the newly formed islets of neocartilage served as an adequate structural support and the process of degradation and neocartilage formation was balanced.

In addition to the mechanical properties, DNSC differs from native cartilage tissue by a significant decrease in the sulfated GAG content, which is reduced during the decellularization procedure.[6] Remarkably, however, neither mechanical properties nor GAG content appeared to be critical for the effective remodeling process and the recruitment of the chondrogenic progenitors, which also occurred in the absence of PDGF-BB loading. This may be partly attributable to the context of the species and/or the anatomical site. Nevertheless, these observations may be useful to take into account when considering critical parameters in the design of synthetic scaffolds for cartilage reconstruction.

Furthermore, DNSC degradation progressed slower in the PDGF-BB group than in the untreated scaffold group. This may be explained by inhibition of the proteolytic degradation of DNSC combined with the enhanced matrix deposition due to the activity of PDGF-BB. Notably, the correlation between matrix degradation and neocartilage formation was also less in the PDFG group as compared to the untreated samples. However, given the dynamics of the process and visible infiltration of the remaining DNSC matrix lacunae, it is reasonable to assume that eventually the DNSC matrix will be fully degraded and could lead to further deposition of neocartilage in long-term. Notably, however, longer experiments might also reveal the initiation of absorption processes.

In conclusion, our study demonstrated that in situ regeneration of septal defects using decellularized septal cartilage scaffolds could be significantly augmented by functionalizing the matrix with recombinant PDGF-BB. Furthermore, the DNSC matrix could provide sufficient support and sustain the septal structure until the deposition of neocartilage tissues during the evaluation period used in this study. It should be noted, however, that increasing the study group size and prolonging the duration of the evaluation period are required to confirm the stability of the remodeling process, as well as the long-term viability of the formed neocartilage tissue observed in our experiments. Furthermore, while PDFG-BB is approved for clinical use in some countries,[25] the translation of products functionalized with this cytokine into clinical setting might be hampered by regulatory hurdles elsewhere. Overall, however, our study opens a new perspective for in situ regenerative therapy of nasal cartilage defects using a cell-free, biocompatible, and readily accessible xenogeneic matrix.

ORCID iDs

Huber Lena https://orcid.org/0000-0002-0252-4911
Gvaramia David https://orcid.org/0000-0002-6013-3513
Breiter Roman https://orcid.org/0000-0003-0889-9199

Supplemental material

Supplemental material for this article is available online.

References

1. Gaharwar AK, Singh I and Khademhosseini A. Engineered biomaterials for in situ tissue regeneration. *Nat Rev Mater* 2020; 5: 686–705.
2. Bonnans C, Chou J and Werb Z. Remodelling the extracellular matrix in development and disease. *Nat Rev Mol Cell Biol* 2014; 15: 786–801.
3. Popko M, Bleys RL, De Groot JW, et al. Histological structure of the nasal cartilages and their perichondrial envelope. I. the septal and lobular cartilage. *Rhinology* 2007; 45: 148–152.
4. Lavernia L, Brown WE, Wong BJF, et al. Toward tissue-engineering of nasal cartilages. *Acta Biomater* 2019; 88: 42–56.
5. Schwarz S, Elsaesser AF, Koerber L, et al. Processed xenogenic cartilage as innovative biomatrix for cartilage tissue engineering: effects on chondrocyte differentiation and function. *J Tissue Eng Regen Med* 2015; 9: E239–E251.
6. Schwarz S, Koerber L, Elsaesser AF, et al. Decellularized cartilage matrix as a novel biomatrix for cartilage tissue-engineering applications. *Tissue Eng Part A* 2012; 18: 2195–2209.
7. von Bomhard A, Elsaesser A, Riepl R, et al. Cartilage regeneration using decellularized cartilage matrix: long-term

comparison of subcutaneous and intranasal placement in a rabbit model. *J Craniomaxillofac Surg* 2019; 47: 682–694.
8. Fiedler J, Röderer G, Günther KP, et al. BMP-2, BMP-4, and PDGF-bb stimulate chemotactic migration of primary human mesenchymal progenitor cells. *J Cell Biochem* 2002; 87: 305–312.
9. Fiedler J, Etzel N and Brenner RE. To go or not to go: Migration of human mesenchymal progenitor cells stimulated by isoforms of PDGF. *J Cell Biochem* 2004; 93: 990–998.
10. Elsaesser AF, Bermueller C, Schwarz S, et al. In vitro cytotoxicity and in vivo effects of a decellularized xenogeneic collagen scaffold in nasal cartilage repair. *Tissue Eng Part A* 2014; 20: 1668–1678.
11. Redondo ML, Beer AJ and Yanke AB. Cartilage restoration: microfracture and osteochondral autograft transplantation. *J Knee Surg* 2018; 31: 231–238.
12. Guo T, Noshin M, Baker HB, et al. 3D printed biofunctionalized scaffolds for microfracture repair of cartilage defects. *Biomaterials* 2018; 185: 219–231.
13. Yang Z, Zhao T, Gao C, et al. 3D-bioprinted difunctional scaffold for in situ cartilage regeneration based on aptamer-directed cell recruitment and growth factor-enhanced cell chondrogenesis. *ACS Appl Mater Interfaces* 2021; 13: 23369–23383.
14. Sun X, Yin H, Wang Y, et al. In situ articular cartilage regeneration through endogenous reparative cell homing using a functional bone marrow-specific scaffolding system. *ACS Appl Mater Interfaces* 2018; 10: 38715–38728.
15. Dong Y, Liu Y, Chen Y, et al. Spatiotemporal regulation of endogenous MSCs using a functional injectable hydrogel system for cartilage regeneration. *NPG Asia Mater* 2021; 13: 71.
16. Zhou T, Li X, Li G, et al. Injectable and thermosensitive TGF-β1-loaded PCEC hydrogel system for in vivo cartilage repair. *Sci Rep* 2017; 7: 10553.
17. Hannink M and Donoghue DJ. Structure and function of platelet-derived growth factor (PDGF) and related proteins. *Biochim Biophys Acta* 1989; 989: 1–10.
18. Andrae J, Gallini R and Betsholtz C. Role of platelet-derived growth factors in physiology and medicine. *Genes Dev* 2008; 22: 1276–1312.
19. Joos H, Wildner A, Hogrefe C, et al. Interleukin-1 beta and tumor necrosis factor alpha inhibit migration activity of chondrogenic progenitor cells from non-fibrillated osteoarthritic cartilage. *Arthritis Res Ther* 2013; 15: R119.
20. Evrova O and Buschmann J. In vitro and in vivo effects of PDGF-BB delivery strategies on tendon healing: a review. *Eur Cell Mater* 2017; 34: 15–39.
21. Lee J, Yoo JJ, Atala A, et al. The effect of controlled release of PDGF-BB from heparin-conjugated electrospun PCL/gelatin scaffolds on cellular bioactivity and infiltration. *Biomaterials* 2012; 33: 6709–6720.
22. Judith R, Nithya M, Rose C, et al. Application of a PDGF-containing novel gel for cutaneous wound healing. *Life Sci* 2010; 87: 1–8.
23. Hsieh PC, Davis ME, Gannon J, et al. Controlled delivery of PDGF-BB for myocardial protection using injectable self-assembling peptide nanofibers. *J Clin Invest* 2006; 116: 237–248.

24. Hsieh PC, MacGillivray C, Gannon J, et al. Local controlled intramyocardial delivery of platelet-derived growth factor improves postinfarction ventricular function without pulmonary toxicity. *Circulation* 2006; 114: 637–644.

25. Steed DL. Clinical evaluation of recombinant human platelet-derived growth factor for the treatment of lower extremity ulcers. *Plast Reconstr Surg* 2006; 117: 143S–149S. discussion 150S-151S.

26. Alkindi M, Ramalingam S, Alghamdi O, et al. Guided bone regeneration with osteoconductive grafts and PDGF: a tissue engineering option for segmental bone defect reconstruction. *J Appl Biomater Funct Mater* 2021; 19: 2280800020987405.

27. Pierce GF, Mustoe TA, Altrock BW, et al. Role of platelet-derived growth factor in wound healing. *J Cell Biochem* 1991; 45: 319–326.

28. Hanaoka K, Tanaka E, Takata T, et al. Platelet-derived growth factor enhances proliferation and matrix synthesis of temporomandibular joint disc-derived cells. *Angle Orthod* 2006; 76: 486–492.

29. Montaseri A, Busch F, Mobasheri A, et al. IGF-1 and PDGF-bb suppress IL-1β-Induced cartilage degradation through down-regulation of NF-κB signaling: involvement of Src/PI-3K/AKT pathway. *PLoS One* 2011; 6: e28663.

30. Kim YK, Chen EY and Liu WF. Biomolecular strategies to modulate the macrophage response to implanted materials. *J Mater Chem B* 2016; 4: 1600–1609.

31. Aamodt JM and Grainger DW. Extracellular matrix-based biomaterial scaffolds and the host response. *Biomaterials* 2016; 86: 68–82.

32. Kzhyshkowska J, Gudima A, Riabov V, et al. Macrophage responses to implants: prospects for personalized medicine. *J Leukoc Biol* 2015; 98: 953–962.

33. Sridharan R, Cameron AR, Kelly DJ, et al. Biomaterial based modulation of macrophage polarization: a review and suggested design principles. *Mater Today* 2015; 18: 313–325.

34. Dong D, Tsao C, Hung HC, et al. High-strength and fibrous capsule-resistant zwitterionic elastomers. *Sci Adv* 2021; 7: eabc5442.

35. Brown BN, Londono R, Tottey S, et al. Macrophage phenotype as a predictor of constructive remodeling following the implantation of biologically derived surgical mesh materials. *Acta Biomater* 2012; 8: 978–987.

36. Badylak SF. Decellularized allogeneic and xenogeneic tissue as a bioscaffold for regenerative medicine: factors that influence the host response. *Ann Biomed Eng* 2014; 42: 1517–1527.

37. Banerjee P and Shanthi C. Cryptic peptides from collagen: a critical review. *Protein Pept Lett* 2016; 23: 664–672.

38. Hussey GS, Dziki JL and Badylak SF. Extracellular matrix-based materials for regenerative medicine. *Nat Rev Mater* 2018; 3: 159–173.

39. Mola F, Keskin G, Ozturk M, et al. The comparison of acellular dermal matric (Alloderm), Dacron, Gore-Tex, and autologous cartilage graft materials in an experimental animal model for nasal septal repair surgery. *Am J Rhinol* 2007; 21: 330–334.